Electron Microscopy of Wet Tissues: A Case Study in Renal Pathology

ABRAHAM NYSKA,[1] CONNIE A. CUMMINGS,[2] ANYA VAINSHTEIN,[3] JONATHAN NADLER,[4] NATHAN EZOV,[4]
YONA GRUNFELD,[4] OPHER GILEADI,[3] AND VERED BEHAR[3]

[1]*Laboratory of Experimental Pathology, National Institute of Environmental Health Sciences (NIEHS),*
Research Triangle Park, North Carolina 27709, USA
[2]*Pathology Associates (PAI) Division of Charles River Laboratories, Inc., Durham, North Carolina 27713, USA*
[3]*QuantomiX, Ltd., Nes Ziona 70400, Israel, and*
[4]*Harlan Biotech Israel Ltd., Kiryat Weizmann, Rehovot 76326, Israel*

ABSTRACT

In this report we introduce wet-tissue scanning electron microscopy, a novel technique for direct imaging of wet tissue samples using backscattered electrons. Samples placed in sealed capsules are imaged through a resilient, electron-transparent membrane. The contrast of the imaged samples may be enhanced by chemical staining. The samples several millimeters thick and imaged without sectioning, makes this technique suitable for rapid analysis of tissue specimens. We applied this technique to D-limonene-induced nephropathy where accumulation of hyaline protein droplets is induced in proximal and distal convoluted tubules of the kidney. Images obtained by scanning electron microscopy of hydrated kidney specimens exhibited superior resolution, contrast, and magnification compared with those obtained by conventional light microscopy of paraffin sections. The electron micrographs can be obtained within an hour of tissue removal, whereas preparation for light microscopy requires at least 1 day. These advantages of the wet scanning electron microscopy technique indicate its potential utility in a wide range of applications in histopathology and toxicology.

Keywords. Scanning electron microscopy; imaging; wet samples; kidney.

INTRODUCTION

Modern advances in imaging and immunolabeling techniques for light microscopy (LM) and electron microscopy (EM) have contributed to resolution enhancement and improved diagnostic accuracy. Light microscopic resolution is limited by diffraction of about 0.2 microns; the use of transmission EM (TEM) is encumbered by extensive processing that requires skill and a period of several days to achieve and may alter structure of the sample significantly. The ultrathin sections (90 nm) that are usually imaged by TEM represent a limited and often arbitrary portion of the sample necessitating the imaging of multiple serial sections at different depths within the tissue. Scanning electron microscopy (SEM), usually restricted to surface imaging, allows only the restrictive investigation of surface topography, while imaging of intracellular structure requires specialized preparatory techniques, such as fracturing and etching.

A recent review (Tucker, 2000) discusses modes of clinical diagnoses in which a small but significant proportion of cases (3–8%), especially of cancer and nonneoplastic renal diseases, can be identified solely by EM (Gyorkey et al., 1975; Spargo, 1975; Eddy, 1989, 2001; Tucker, 2000; Gu and Herrera, 2002). These numbers probably underestimate the potential contribution of EM, since its usage is limited not only by lack of utility in many clinical situations, but also by cost, time required to produce results, and relatively low output compared to that of histological methods. A significant need exists, therefore, for an imaging system for biological tissues and cells that achieve EM resolution with sample-preparation procedures comparable to those of LM.

We present wet SEM, a technique that allows high-resolution imaging of wet biological samples in a scanning electron microscope at atmospheric pressure and any desired temperature. The sample, placed in a sealed specimen capsule, is separated from the vacuum by a thin, electron-transparent partition membrane (Figure 1) that allows the penetration of electrons and the collection of backscattered electrons while withstanding a pressure difference of one atmosphere. Unlike conventional SEM and similar techniques, the sample is completely isolated from the vacuum within the microscope. Consequently, there is no loss of water or change in material composition in the sample during preparation or imaging. While the technique can be applied to a variety of biological and other wet specimens (e.g., tissue culture, sperm cells, bacteria, and protozoa), the present work describes in detail its specific application to the analysis of pathological changes in renal tissue.

We chose the analysis of kidney pathology as a subject for wet SEM for three reasons. Since renal pathology is one of the few remaining areas in which EM is still widely used for diagnostic purposes, the application of wet SEM may offer an alternative, significantly simplified method to achieve high-resolution imaging. Because the kidney is targeted for toxicity by a wide variety of agents and adversely affected by many disease states, our imaging technology may enhance the sensitivity and/or precision of analyses. In addition, since various normal and pathological structures can be visualized in kidney pathology, the wet SEM will likely provide a firm basis for investigation of other tissues.

D-Limonene is representative of a large group of substances that cause the accumulation of hyaline droplets, a classical pathology in kidneys of male rats. (Lehman-McKeeman et al.,

1A
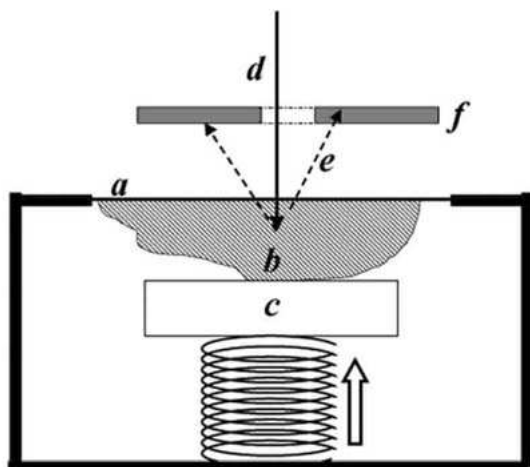
1B

FIGURE 1.—Depiction of the specimen capsule used for imaging of wet samples in scanning electron microscope. A: schematic cross-sectional view of the capsule enclosing a tissue sample. The generally rigid capsule is topped by a window covered by an electron-transparent partition membrane (a). The tissue (b) is held in close contact with the membrane by a spring-supported plunger (c). When placed in the evacuated chamber of the microscope, the tissue is maintained in an aqueous state at atmospheric pressure. A microscopic image is obtained when the scanning electron beam (d) penetrates the partition membrane, interacts with the sample, and backscattered electrons (BSE) (e) are detected by a BSE detector (f). B: external view.

1989). Although this phenomenon is not known to appear in humans or other animals, including female rats, it has proved to be a useful parameter in toxicological studies and models of carcinogenicity in rats (Hard, 1998). With administration of sufficient doses of D-limonene to male rats, $\alpha_{2\mu}$ globulin has been found to accumulate excessively in the P2 segment cells of renal proximal tubules, resulting in hyaline droplet formation as a manifestation of protein overload. Hyaline droplet accumulation is the first stage in a unique sequence occurring in nephropathies (also known as $\alpha_{2\mu}$-globulin nephropathy), including granular casts in the outer medulla and linear mineralization in the papilla. We have chosen this model since it presents a well-defined structural pattern in the kidney tissue,

demonstrates the explorative abilities of this technique, and emphasizes improved accuracy of detection. The wet SEM technique may provide significant improvement in the diagnostic accuracy in renal toxicological pathology as well as tumor pathology.

METHODS

Chemicals and Solutions

Paraformaldehyde (16%, EM grade), glutaraldehyde (25%, EM grade), uranyl acetate, and tannic acid were obtained from Electron Microscopy Sciences (Fort Washington, PA). Corn oil and D-limonene were purchased from Sigma-Aldrich (St. Louis, MO).

Flushing Solution: 1 ml heparin (1000 units/ml), 1 ml 1% sodium nitrate, and 8.5 g NaCl in 1 L deionized H_2O were used to flush blood from the circulation before perfusion with the fixative.

Fixative Solution: 710 ml deionized H_2O, 250 ml 16% paraformaldehyde, 40 ml 25% glutaraldehyde, and 11.6 g $NaH_2PO_4 \cdot H_2O$, pH adjusted to 7.2–7.4 (McDowell and Trump, 1976) constituted the fixative perfusate.

Uranyl Acetate: A 5% (w/v) stock solution, pH 3.5, was diluted just before use in water to the desired concentration (0.1%) for application of an electron-dense stain to the samples.

Animal Treatment

Male Sprague–Dawley rats (11–13-weeks-old) were obtained from Harlan Laboratories (Jerusalem, Israel), maintained on Harlan Teklad TRM Rat/Mouse Diet and water provided ad libidum, and allowed a 3-week acclimation period to facility conditions (19–25°C, 30–70% relative humidity, and a 12-hour light/dark cycle) prior to inclusion in the study. All procedures, care, and treatment of rats were in accordance with the principles of humane treatment outlined by the *Guide for the Care and Use of Laboratory Animals* of the National Institutes of Health (National Research Council, 1996). The study was conducted following the review and approval of the Committee for Ethical Conduct in the Care and Use of Laboratory Animals and after being found in compliance with the rules and regulations set forth. D-Limonene (800 mg/kg in corn oil) was administered once by oral gavage to 2 rats, while a control rat was administered 10 ml/kg of corn oil. The animals were observed daily for abnormal clinical signs and weighed just prior to the first dosing and at study termination.

Perfusion, Necropsy, and Tissue Handling

At 48 hours postdosing and following full anesthesia with sodium pentobarbitone, animals were subjected to whole-body vascular perfusion with buffered glutaraldehyde-formaldehyde fixative (McDowell and Trump, 1976; Dykstra et al., 2002) applied by gravitational force with the container placed approximately 1 m above the body of the animal. Whole-body vascular perfusion was administered by a cannula passed through the left ventricle to the aorta. Initially, the vascular system was flushed with the flushing solution for approximately 10–15 minutes or until the liver appeared pale.

Immediately following flushing, the solution was changed to the fixative solution, and perfusion was continued until the entire body became rigid (approximately 400 ml/animal). Thereupon both kidneys were excised, immersed in the same fixation medium, and transferred to a vial containing fixative until further processing.

Each kidney was cut longitudinally into approximately 0.5-mm slices using a vibratome to produce smooth internal surfaces, and each slice was then cut transversely into 2 halves. One of these, further processed for wet EM, received direct staining with 0.1% uranyl acetate. The other that was processed for light microscopic histopathology was embedded in paraffin, sectioned at 5–6 μm, and stained with hematoxylin and eosin (H&E) and Mallory-Heidenhain (MH) (Bancroft and Gamble, 2001).

Sample Preparation for Wet Scanning Electron Microscopy

General Considerations: A wide variety of sample preparation procedures are suitable for wet tissue SEM. The sample presented for imaging must have a relatively smooth surface, which can either be the natural edge of the tissue or be generated by cutting; the tissue should be sufficiently soft to lay flush against the partition membrane; and the sample should display some contrast for imaging. Although samples can be imaged without fixation, this step is preferred to prevent autolysis and preserve structural integrity. Fixation is subject to the same considerations that apply to histopathology in general; rapid and efficient penetration of the fixative is ensured either by vascular perfusion or by immersing thin (2–3 mm or less) tissue fragments in the fixative solution. Samples are generally not embedded in paraffin or resin and are sliced to a thickness of up to 2 mm either manually with a razor blade or a mechanical tissue slicer. Imaging in the SEM is restricted by the penetration of the electron beam to a depth of several microns from the surface. Consequently, staining can be performed rapidly, just to allow the stain to penetrate to the relevant depth of a few microns. Contrast in backscattered electron images is mostly dependent on the distribution of materials with different atomic numbers. Native material differences within the sample generate some contrast, but usually a heavy metal stain, such as uranyl acetate or osmium tetroxide, is used to enhance contrast.

Specific Protocol: In the experiment described in this work, fixed tissue fragments were rinsed extensively in water; treated with 1% tannic acid for 5 minutes; rinsed in water; stained with 0.1% uranyl acetate, pH 3.5, for 10 minutes; then washed several times with water. Stained samples were maintained at 4°C.

SEM Imaging

For wet SEM, specimens are routinely trimmed to a diameter of up to 3 mm and a thickness of up to 2 mm to fit the internal dimensions of the QX-302 capsule (QuantomiX, Ltd., Nes Ziona, Israel). The sample was placed in the capsule with the surface to be imaged in close contact with the partition membrane. The capsule may contain 5–10 μl of liquid before inserting the specimen. The capsule is sealed so that the plunger maintains the sample in close contact with the membrane. For samples that are thinner than 1 mm, a silicon rubber disc of 2 mm diameter and 1 mm thickness is inserted between the plunger and the sample.

The sealed capsule is then placed on the specimen stage of the SEM, and vacuum is applied. Imaging is performed according to the operating instructions of the SEM, with attention given to some features that may differ from standard imaging modes. Imaging is done using a backscattered electron detector. In addition, the electron beam energy should be at least 15 kV, and typically 30 kV. Imaging is performed at higher current (spot size) and slower scan rate to compensate for the relatively low contrast. Since the capsule is taller than a standard specimen stub, the specimen stage must be adjusted to ensure an optimal working distance. The specific settings vary between microscopes and between different specimens. The images presented in this work were obtained on a FEI XL-30 ESEM microscope with a working distance of 8 mm, beam energy of 15–30 kV, spot size of 4–5 (beam current of 200–800 pA), and scan rates of 1.3–120 msec/line at 484 lines/frame.

RESULTS

Figure 1 depicts the specimen capsule used for imaging wet samples in a scanning electron microscope. Figure 1A presents a schematic cross-sectional view of the capsule enclosing a tissue sample; Figure 1B shows an external view. The capsule encloses an internal volume, which can hold a tissue fragment of up to approximately 3 mm, immersed in liquid and completely isolated from the vacuum in the SEM chamber. The imaging window (a in Figure 1A) is 3 mm in diameter and covered by an electron-transparent partition membrane; the spring-supported plunger c assures that the tissue is in good contact with the partition membrane.

Figures 2A and B, are photomicrographs of kidney sections from a control animal, and Figure 3A and B—from a D-limonene-treated animal (A—H&E staining and B—MH staining). Histologically, the accumulation of hyaline droplets was recognized chiefly by bright round eosinophilic deposits within the tubular epithelium. The hyaline droplets were visible as pale-orange bodies in H&E-stained sections (Figure 3A, arrows) and more clearly visualized as bright orange-colored bodies by MH staining (Figure 3B, arrows). In treated animals, hyaline droplets were occasionally angular to elongated and often filled individual tubular epithelial cells. In general, these droplets occurred more commonly in the proximal convoluted tubules. While control animals displayed randomly scattered droplets with a minimal accumulation, treated rats exhibited a mild to moderate increase in the number of hyaline droplets within tubular epithelium, compared with the numbers seen in tubules of controls. Other histologic findings included randomly scattered individual tubules undergoing early necrosis and tubular-cast formation in treated rats.

Parallel segments from the same kidneys were visualized in a scanning electron microscope using the wet SEM methodology. Proximal and distal convoluted tubule (Figures 2C, 2D, 3C, and 3D) appeared quite simple to differentiate. Likewise, individual organelles, such as mitochondria, tubular epithelial nuclei; the brush border of the proximal convoluted tubule; and protein/hyaline droplets were easily detected. Most often round, but occasionally variable in size and shape, intensely
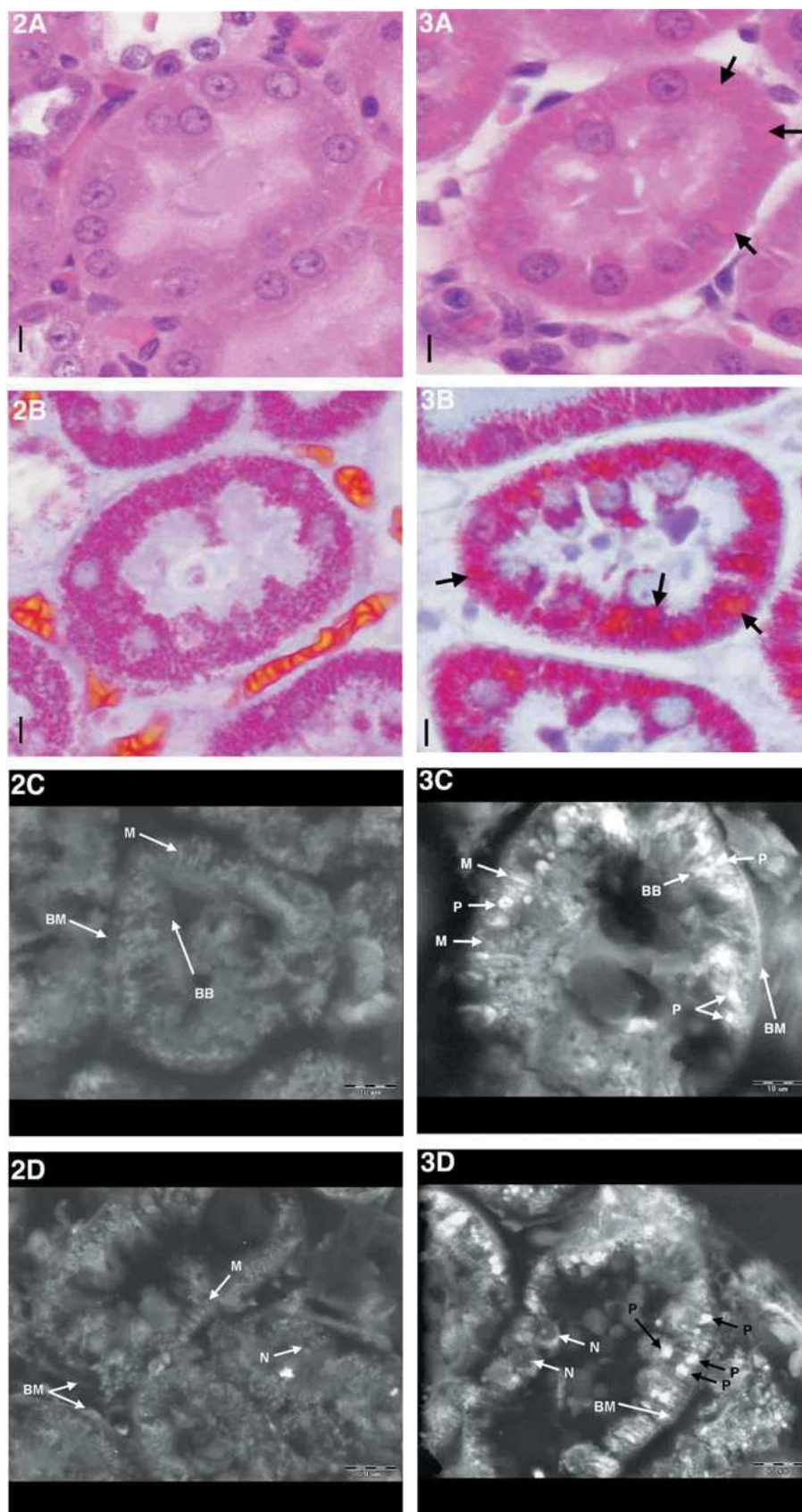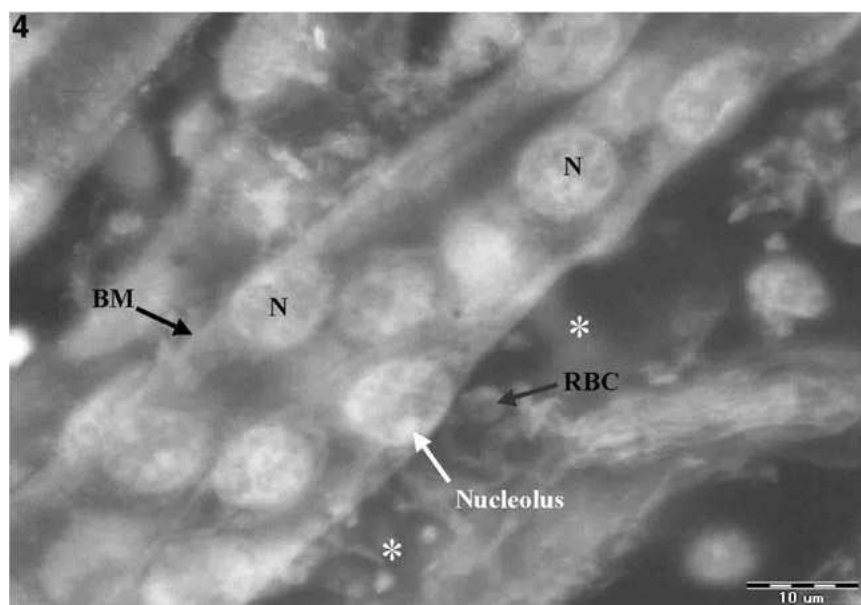
FIGURE 4.—Kidney section from control animal viewed using wet scanning electron microscopy showing normal aspects of the medullary collecting tubule. BM = basement membrane, N = nucleus, RBC = red blood cell, asterisks mark peritubular blood capillaries. Bar = 10 μm.

bright, white electron-dense deposits were clearly defined within the cytoplasm of the epithelial cells lining individual tubules. These particular deposits were brightly eosinophilic following MH staining (Figure 3B). Figures 2C and D present images of the kidney of an untreated animal; note the absence of the bright hyaline droplets.

Figures 4 and 5 depict electron micrographs of 2 additional regions from the kidneys of control animals. Figure 4 reveals an area of the medulla in which the epithelium of a collecting tubule is seen with subcellular detail. Figure 5 shows a glomerulus with podocytes, urinary space, mesangial matrix, and basement membrane.

DISCUSSION

The initial impetus for the development of the wet SEM technique was to achieve high-resolution images of biological specimens while minimizing the complexity of sample preparation. We demonstrated that the ability to image stable, wet samples in the electron microscope allows the investigator to exceed the fundamental limits of resolution and magnification of LM. Images visible by scanning electron microscopy of wet kidney specimens were obtained quickly, within an hour of tissue removal, and exhibited superior resolution, contrast, and magnification compared with those revealed by

conventional LM of paraffin sections. In addition, numerous features of the wet SEM methodology provide the investigator with a novel tool that allows a rapid, accurate pathological analysis. Because of the structure of the capsule and mode of detection, the sample can be maintained in a fully aqueous state, without dehydration or drying, and imaged stably in the electron microscope to allow the fundamental limits of resolution and magnification of LM to be exceeded. The wet SEM technology is conceptually different from other approaches to SEM imaging of wet samples, such as environmental or low-vacuum SEM, in that the sample is completely isolated from the vacuum compartment and special conditions, such as low temperature or precise control of water vapor pressure, are not needed to prevent sample dehydration. Indeed, the wet SEM techniques allows the sample to retain its structure and composition for prolonged periods at atmospheric pressure and any desired temperature.

Since the aqueous state of the sample eliminates charging artifacts, coating with an extraneous conductive layer is not necessary. With image formation based on the detection of backscattered electrons, within a thin layer (up to 2–3 μm) of the sample obtained without actual sectioning, internal features can be revealed. In contrast, in traditional SEM imaging that uses secondary-electron detection, features can be observed only on the surface of the sample. This wet procedure,

---

Figures 2–3

FIGURE 2.—Kidney sections of a control rat. (A) Section of the proximal tubule of the cortex stained by hematoxylin & eosin and viewed by light microscopy. Bar = 10 μm; (B) Section of the proximal tubule of the cortex stained by Mallory-Heidenhain and viewed by light microscopy. Bar = 10 μm; (C) Section of the proximal convoluted tubule viewed using wet scanning electron microscopy. Note the general absence of the bright, white electron-dense deposits (hyaline droplets) evident in kidneys of treated animals. M = mitochondria, BB = brush border, BM = basement membrane, N = nuclei. Bar = 10 μm. (D) Section of the distal convoluted tubule. Bar = 20 μm. 3.—Kidney sections of a D-limonene (800 mg/kg)-treated rat. (A) Section of the proximal tubule of the cortex stained by hematoxylin & eosin and viewed by light microscopy. Hyaline droplets marked with arrows. Bar = 10 μm; (B) Section of the cortex–proximal tubule, stained by Mallory-Heidenhain and viewed by light microscopy. Hyaline droplets marked with arrows. Bar = 10 μm; (C) Section of the proximal convoluted tubule viewed using wet scanning electron microscopy. Note the bright, white electron-dense deposits, hyaline protein droplets (P). M = mitochondria, BB = brush border, BM = basement membrane, N = nuclei. Bar = 10 μm. (D) Section of the distal convoluted tubule. Note the bright, white electron-dense deposits, hyaline protein droplets (P). Bar = 20 μm.
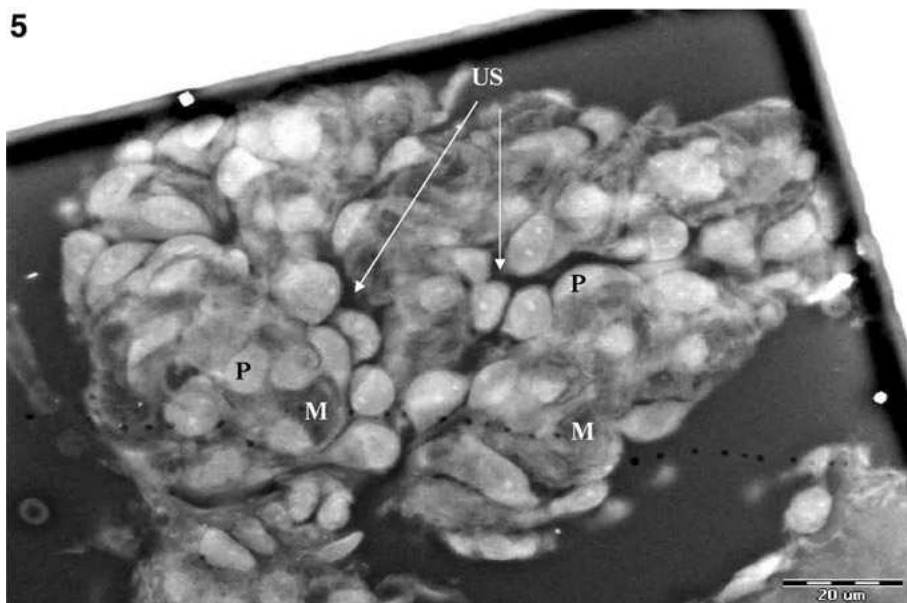
FIGURE 5.—Kidney section from control animal viewed using wet scanning electron microscopy showing normal aspects of the glomerulus. US = urinary space, P = podocyte nucleus, M = mesangial matrix. Bar = 20 μm.

allowing samples of several-millimeters thickness to be imaged without thin sectioning, eliminates the need for paraffin or resin embedding or cryosectioning. A natural edge of a tissue specimen, such as an epithelial layer, can be imaged directly, or an internal surface may be exposed by cutting the wet tissue with a scalpel or vibratome. Regions beyond the layer under examination have no effect on imaging. The most difficult and time-consuming aspects of conventional histological sample preparation are embedding and sectioning. The entire wet SEM procedure, from fixed tissue to image acquisition, usually requires less than one hour, compared to at least a day needed for paraffin embedding, sectioning, paraffin removal, and staining for LM.

Another feature distinguishing the wet SEM technique from conventional histopathologic methodologies is the use of different contrast agents, mostly electron-dense stains, which can better distinguish some features, exemplified by the hyaline protein droplets that were clearly visible. In addition to identifying the increase in hyaline protein droplets, many additional features can be seen in wet SEM images, including subcellular organelles and extracellular structures, such as basement membranes. These observations indicate that the wet SEM technique will likely prove valuable in the analysis and diagnosis of a wider variety of nephropathies.

Existing histopathologic techniques are supported by an extensive body of literature and practical experience. Introduction of a new procedure that produces different images requires documentation of some advantage—in the quality of the resulting information or in the reduction in time, complexity, or expense involved. The wet SEM technology offers such advantages, especially in simplification of sample preparation, compared to methods for conventional LM and EM. The technique yields significant improvements in magnification and visibility of fine details over those obtained by histological methods. In addition, the contrast mechanisms reveal information that is qualitatively different and may highlight specific features of interest. The images of medullary collecting tubules (Figure 4) and a glomerulus (Figure 5) indicate the wider potential of the wet SEM technique for histopathological analysis. Images with magnification and resolution of detail that surpass the capabilities of LM can be obtained at a fraction of the time required for standard paraffin sections.

We have presented in Figures 2A, 2B, as well as 3A, and 3B parallel analyses of the same tissues using conventional LM and wet SEM. Such comparisons serve as a necessary validation of a new technique and to reveal its potential advantages. In this case, higher magnification and contrast and the concurrent imaging of protein droplets with subcellular organelles and extracellular structures demonstrate the benefits of this methodology. A similar combination of images obtained by different methods may constitute a powerful approach in some investigations. The wet SEM technique will allow the incorporation of high-resolution data on a more routine basis than is currently available with existing approaches. Our demonstration of the utility of the wet SEM technique for a specific toxicological application indicates the potential for expanding its capabilities to a wider range of pathologies and biomedical observations.

REFERENCES

Bancroft, J. D., and Gamble, M. G. (2001). Theory and Practice of Histochemical Techniques. 5th edition. Harcourt Health Sciences, New York.

Dykstra, M. J., Mann, P. C., Elwell, M. R., Ching, S. V. (2002). Suggested standard operating procedures (SOPs) for the preparation of electron

microscopy samples for toxicology/pathology studies in a GLP environment. *Toxicol Pathol* **30**, 735–43.

Eddy, A. A. (1989). Interstitial nephritis induced by protein-overload proteinuria. *Am J Pathol* **135**, 719–33.

Eddy, A. A. (2001). Role of cellular infiltrates in response to proteinuria. *Am J Kidney Dis* **37**, S25–9.

Gu, X., and Herrera, G. A. (2002). The value of electron microscopy in the diagnosis of IgA nephropathy. *Ultrastruct Pathol* **26**, 203–10.

Gyorkey, F., Min, K. W., Krisko, I., and Gyorkey, P. (1975). The usefulness of electron microscopy in the diagnosis of human tumors. *Hum Pathol* **6**, 421–41.

Hard, G. C. (1998). Mechanisms of chemically induced renal carcinogenesis in the laboratory rodent. *Toxicol Pathol* **26**, 104–12.

Lehman-McKeeman, L. D., Rodriguez, P. A., Takigiku, R., Caudill, D., and Fey, M. L. (1989). D-Limonene induced male rat-specific nephrotoxicity: evaluation of the association between D-limonene and $\alpha_{2\mu}$-globulin. *Toxicol Appl Pharmacol* **99**, 250–9.

McDowell, E. M., and Trump, B. F. (1976). Histologic fixatives suitable for diagnostic light and electron microscopy. *Arch Pathol Lab Med* **100**, 405–14.

National Research Council (1996). *Guide for the Care and Use of Laboratory Animals*. National Academy Press, Washington, DC.

Spargo, B. H. (1975). Practical use of electron microscopy for the diagnosis of glomerular disease. *Hum Pathol* **6**, 405–20.

Tucker, J. A. (2000). The continuing value of electron microscopy in surgical pathology. *Ultrastruct Pathol* **24**, 383–9.